Catalysis Today 151 (2010) 107–113

Contents lists available at ScienceDirect

Catalysis Today

journal homepage: www.elsevier.com/locate/cattod

Degradation study of 15 emerging contaminants at low concentration by immobilized TiO_2 in a pilot plant

N. Miranda-García[a], M. Ignacio Maldonado[a,*], J.M. Coronado[b], Sixto Malato[a]

[a] Plataforma Solar de Almería, CIEMAT, Carretera Senés, Km 4, 04200 Tabernas, Almería, Spain
[b] IMDEA-Energía, Universidad Rey Juan Carlos – Laboratorio III, 28933 Mostoles, Madrid, Spain

ARTICLE INFO

Article history:
Available online 14 April 2010

Keywords:
Emerging contaminants
Immobilized photocatalyst
Solar pilot plant
Solar photocatalysis
Wastewater reuse

ABSTRACT

The purpose of this study was to develop a municipal wastewater treatment method based on a solar advanced oxidation process (AOP) permitting reuse of the treated wastewater. The photoactive layer of TiO_2 was deposited on glass spheres using the sol–gel dip-coating technique. The film was characterized by X-ray diffraction and scanning electron microscopy (SEM). Degradation of 15 emerging contaminants (ECs), each with an initial concentration of 100 $\mu g\,L^{-1}$ was determined by ultra-performance liquid chromatography (UPLC–UV) and mineralization was monitored by measuring the dissolved organic carbon (DOC). The experiments were performed in a pilot compound parabolic collector (CPC) solar plant at the Plataforma Solar of Almeria. Five cycles of photocatalysis were studied for photocatalyst durability and activity. It was demonstrated that after five cycles, although photoactivity of the catalyst slowly decreases, it continues degrading contaminants.

1. Introduction

With water exploitation rates (annual consumption/resources) of over 20%, Spain has the highest water deficit in Europe, and this is generating serious social concern. Although Spain is also one of the countries with the most reuse of water, this percentage is still very low. At present, only 5% of wastewater is reused [1].

Municipal wastewater treatment plants (MWTPs) are a major source of water for potential reuse. However, quality demands for reusable water [2–4] require that it not contain any toxic which escape conventional wastewater treatment [5,6]. Today, what are known as "emerging contaminants" (ECs) are causing particular concern, due to their potential effects on health, and data regarding their occurrence [7,8]. It could be emphasized the growing problem of continuously rising concentrations of these non-biodegradable compounds [9–12]. They are resistant to conventional wastewater treatments, and are found in their effluents at concentrations ranging from 0.1 to 20.0 $\mu g\,L^{-1}$ [13,14]. For water to be reusable, it must be free of these emerging contaminants [5,6].

These ECs have different adverse effects in the environment such as aquatic environment, surface water, drinking water or soil, and represent a threat for the humans. Endocrine-disrupting compounds interfere with the normal functioning of the endocrine system [15,16].

Advanced oxidation processes (AOPs), generally defined as water treatment technologies generating hydroxyl radicals which are responsible for organic degradation, due to their strong unselective oxidative power, are able to oxidize and mineralize almost any organic molecule, yielding CO_2 and inorganic ions as final products [18–20], and may therefore be used to remove these contaminants [17].

Although, in general, AOPs are cheap to install, they are expensive to operate, due to the usage of costly chemicals like hydrogen peroxide, increased energy consumption, etc. Use of catalysis and renewable energy resources to power these processes, as in the case of solar photocatalysis, would cut down treatment costs and make AOPs more attractive to the water industry. Future applications of these processes could be improved through the use of immobilized reusable catalysts and solar energy. Therefore, research is focusing increasingly [21] on the AOPs which can be powered by solar radiation (i.e., light with a wavelength over 300 nm), and in particular, heterogeneous photocatalysis with UV/TiO_2.

So far, two forms of TiO_2 have been investigated for photocatalytic degradation processes, in suspension and immobilized on inert-solid supports. Although TiO_2 in suspension (slurry) is usually accepted [22] as more efficient for photocatalytic degradation in water, it must be filtered from the treated effluent, while immobilized TiO_2 has many practical advantages. For example, it does not require downstream separation of the particles from the treated water and the catalyst may be reused for long periods of time, justifying their relatively expensive synthesis. Indeed, the recycling of photocatalyst slurries has proved difficult and uneconomical, especially in wastewater [23–25]. To maximize utilization of the TiO_2

* Corresponding author. Tel.: +34 950 387955; fax: +34 950 365015.
E-mail address: mignacio.maldonado@psa.es (M.I. Maldonado).

0920-5861/$ – see front matter © 2010 Elsevier B.V. All rights reserved.
doi:10.1016/j.cattod.2010.02.044

photocatalyst for practical applications, immobilized supports are being developed [26], and in particular, photocatalysts immobilized on films have recently been the focus of attention. The sol–gel method is well-established as a promising and popular technology for the synthesis of transparent porous TiO_2 films [27–29]. Film porosity benefits photoactivity and can be induced by adding surfactants to the sol [30]. However, like other sol–gel-derived TiO_2 films, each dip-coating cycle of these porous photocatalytic films is very thin [29], and therefore photocatalytic activity is poor due to the small amount of crystalline material and suboptimum UV-light utilization across the film [31].

Today, supported TiO_2 is in common use, nevertheless, the selection of the best support is not an easy task, because it must be resistant to oxidizing environments, UV-transparent, generate a low pressure drop and facilitate contaminant/photocatalyst contact. Borosilicate glass has been used as photocatalytic support, because the catalyst adheres well to it and its transparency is suitable (~400–300 nm) for the TiO_2 activation range [32].

The purpose of this paper is therefore the technical evaluation of solar immobilized TiO_2 in an initial approach describing the solar photocatalytic degradation of 15 emerging contaminants (such as pharmaceuticals, pesticides and personal care products) selected from 56 compounds found in MWTP effluents in previous studies, at low concentrations (100 $\mu g\,L^{-1}$ each) using TiO_2 immobilized on glass spheres [14].

2. Experimental

2.1. Reagents

Reagent-grade nitric acid 65%, polyethyleneglycol PEG-600 (MW: 560–640), hydrochloric acid 37% and isopropanol were provided by Panreac. Titanium isopropoxide $Ti(OPr^i)_4$ 97% was supplied by Sigma–Aldrich. Other reagents were analytical grade.

All reagents used for chromatographic analyses such as, acetonitrile, methanol, and ultrapure (MilliQ) water, were HPLC grade. Analytical standards for chromatography analyses were purchased from Sigma–Aldrich. Table 1 shows the 15 compounds used in the study. The photocatalyst was borosilicate glass spheres (Ø = 5 mm) coated with a solution deposited using the dip-coating method as described below.

Distilled water used in the pilot plant was supplied by the Plataforma Solar of Almería (PSA) distillation plant (conductivity < 10 $\mu S\,cm^{-1}$, Cl^- = 0.2–0.3 $mg\,L^{-1}$, NO_3^- < 0.2 $mg\,L^{-1}$, organic carbon < 0.5 $mg\,L^{-1}$).

The mixture of the emerging contaminants was prepared by dissolving 13 of them in methanol at 2.5 $g\,L^{-1}$ (mother solution) and the other two (Flumequine and Keterolac) were dissolved in water at 100 $mg\,L^{-1}$ due to their low solubility in methanol. Different aliquots of these concentrated solutions were then used during the experiments to attain an initial EC concentration of 100 $\mu g\,L^{-1}$ each. DOC from methanol was 12 $mg\,L^{-1}$.

When the tests were performed in the solar simulator, 40 μL of the mother solution in methanol and 1 mL of Flumequine and Keterolac were added to obtain the desired initial concentration. In the pilot plant, 0.4 mL of mother solution in methanol and 10 mL of the solution of Flumequine and Keterolac were added directly into the pilot plant and homogenized by turbulent recirculation for 15 min.

Table 1
List of selected compounds.

Name	Formula	Substance
Acetaminophen	$C_9H_8NO_2$	Analgesic
Antipyrine	$C_{11}H_{12}N_2O$	Analgesic
Atrazine	$C_8H_{14}ClN_5$	Herbicide
Caffeine	$C_8H_{10}N_4O_2$	Stimulant
Carbamazepine	$C_{15}H_{12}N_2O$	Anticonvulsant
Diclofenac	$C_{14}H_{11}Cl_2NO_2$	Anti-inflammatory
Flumequine	$C_{14}H_{12}NFO_3$	Antibiotic
Hidroxybiphenyl	$C_{12}H_{10}O$	Disruptive Substance
Ibuprofen	$C_{13}H_{18}O_2$	Anti-inflammatory
Isoproturon	$C_{12}H_{18}N_2O$	Herbicide
Keterolac	$C_{15}H_{13}NO_3$	Anti-inflammatory
Ofloxacin	$C_{18}H_{20}FN_3O_4$	Antibacterial
Progesterone	$C_{21}H_{30}O_2$	Steroid Hormone
Sulfamethoxazole	$C_{10}H_{11}N_3O_3S$	Antibiotic
Triclosan	$C_{12}H_7Cl_3O_2$	Antibacterial

2.2. Preparation of the catalyst

TiO_2 was synthesized by sol–gel [33]. For a 2-L volume, 13 mL of nitric acid were added to 1.8 L of distilled water with continuous magnetic stirring. Then $Ti(OPr^i)_4$ was added to solution, and stirred at room temperature until total peptization. 20 $mg\,L^{-1}$ polyethyelene glycol solution was prepared in isopropanol. Both solutions were mixed slowly with continuous stirring. The acid sol was dialyzed to a final pH 2.4–2.5. Finally, Degussa P-25 titanium dioxide was added at a concentration of 10 $g\,L^{-1}$. Glass spheres were prepared by dip-coating several times into this sol at a withdrawal rate of 0.8 $mm\,s^{-1}$. Then the spheres were drained, dried at 110 °C for 90 min and calcined at 400 °C for 5 h using a heating rate of 3 °C min^{-1} (see Fig. 1).

2.3. Materials characterization

XRD patterns were recorded on a Seifert XRD 3000P diffractometer using nickel-filtered Cu Kα radiation. The morphology of the coatings was studied in a Hitachi-3400 II (Japan) scanning electronic microscopy (SEM) at a working voltage of 15 kV, and the morphology was studied without coating in high vacuum.

2.4. Preliminary tests in a solar simulator

The main purpose of the first set of the experiments was to check the durability and photoactivity of the immobilized catalyst. For some initial insight into these information of the immobilized catalyst, experiments were done with the 15 ECs under simulated solar radiation in a solar light simulator (Suntest, XLS+ Heraeus, Germany), equipped with a 2.2 kW xenon arc lamp and special filters restricting transmission of light below 290 nm. Lamp power can be adjusted between 250 and 765 $W\,m^{-2}$ in the range of 290–800 nm (9% corresponds to UV radiation in the 290–400 nm range). Dur-

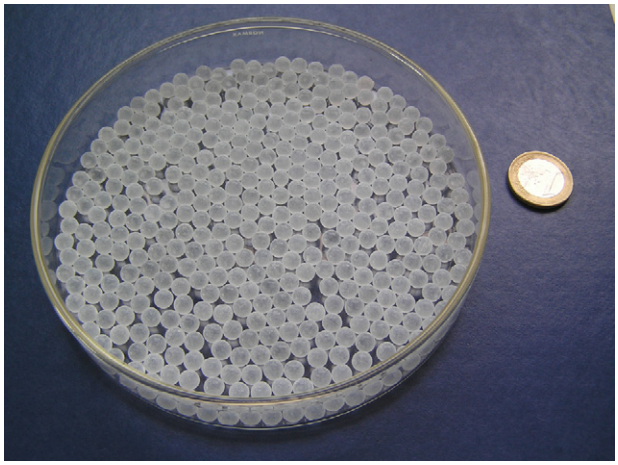

Fig. 1. The spheres (diameter = 5 mm) prepared by sol–gel after calcination.

ing all experiments, the radiation intensity was kept constant at 765 W m^{-2} between 290 and 800 nm (68.85 W m^{-2} in the UV range) and temperature was monitored, varying between 30 and 36 °C.

For these experiments, a peristaltic pump and a Pyrex glass tube, similar to those used in the solar pilot plant CPCs were used. The 20-cm long, 2.5 cm inner-diameter Pyrex glass tube absorbed all photons below 300 nm. The total reactor volume was 1 L (V_T), and irradiated volume 0.07 L (V_i). The pump flow is 1.0 L min^{-1}. For this test, 115 g of spheres (catalyst plus support) were inserted in the reactor. About 0.9 mg of TiO_2 were coated on each sphere by the sol–gel method, however, after washing to remove any trace of the solution, around 0.5 mg of TiO_2/sphere was left. To compare these data with those from the solar pilot plant, they were standardized by Eq. (1), where t_n is the experiment time for each sample. In this case, UV power was not taken into account as the lamp power was constant.

2.5. Solar experimental setup

All solar photochemical experiments were performed in a pilot compound parabolic collector (CPC) plant designed for solar photocatalytic applications. The reactor is composed of two modules of 12 Pyrex glass tubes mounted on a fixed platform tilted 37° (local latitude). For these experiments the usual configuration was changed to use only two glass tubes which they were packed with the glass spheres in a uniform way. The total illuminated area of 0.30 m^2 and total volume (V_T) of 10 L, 0.96 L of which were irradiated volume (V_i) (Fig. 2). The pump flow is 3.65 L min^{-1}. Solar ultraviolet radiation (UV) was measured by a global UV radiometer (KIPP&ZONEN, model CUV 4) mounted on a platform tilted 37°. A plant diagram has been published elsewhere [34]. To compare data from several days' experiments and with other photocatalytic devices, the data were standardized by using Eq. (1), where t_n is the experimental time for each sample, UV is the average solar ultraviolet radiation ($\lambda < 400$ nm) measured between t_{n-1} and t_n, and $t_{30\,W}$ is a "normalized illumination time". In this case, time refers to a constant solar UV power of 30 W m^{-2} (typical solar UV power on a perfectly sunny day around noon).

$$t_{30\ W,n} = t_{30\,W,n-1} + \Delta t_n \frac{UV}{30}\frac{V_i}{V_T}; \quad \Delta t_n = t_n - t_{n-1}; \quad t_0 = 0\,(n=1) \tag{1}$$

The CPC reactor was run several times with distilled water after placing the spheres in it in order to eliminate unattached or weakly bonded TiO_2 particles. At the beginning of the process, when the collectors were covered, the pH was unadjusted. The EC mixture (100 μg L^{-1} each) was added directly into the pilot plant tank and properly homogenized in the dark by turbulent recirculation for 15 min. After homogenization, the solar collectors were discovered and the experiment began.

3. Analytical determinations

Mineralization was monitored by measuring the dissolved organic carbon (DOC) by direct injection of samples filtered with 0.2 μm syringe-driven filters into a Shimadzu-5050A TOC analyzer calibrated with standard solutions of potassium phthalate and provided with a NDIR detector.

The concentration profile of each compound during degradation was determined by UPLC–UV (series 1200, Agilent Technologies, Palo Alto, CA) using a method specifically developed for this application adapted from Martínez-Bueno et al. [14]. Analytes were separated using a reversed-phase C-18 analytical column (Agilent XDB-C18 1.8 μm, 4.6 mm × 50 mm) using acetonitrile (mobile phase A) and ultrapure water (25 mM formic acid, mobile phase B) at a flow rate of 1 mL min^{-1}. A linear gradient progressed from 10% A (initial conditions) to 82% A in 12 min with 3 min. reequilibration time. 25 mL sample was filtered through a 0.2 μm syringe-driven filter, and the filter was washed with 3 mL acetronitrile in order to remove any adsorbed compounds. The two solutions were mixed and a 100 μL aliquot was injected into the UPLC. The UV signal was recorded at different wavelengths according to the wavelength of maximum light absorption of each compound with the response limits of detection (LODs) and limits of quantification (LOQs) [35].

4. Results and discussion

As the purpose of this study was to asses the feasibility of using immobilized TiO_2 for reuse of MWTP effluents, the first step was to test the durability and photoactivity of immobilized TiO_2 on glass spheres in a solar simulator, where very long experiments at constant irradiation power could be performed. Moreover, by this procedure, the new photocatalyst could be tested on a small scale, avoiding the preparation of large quantities until the most suitable could be found. As mentioned in the introduction, the typical concentration of ECs in MWTP effluents is in the 0.1–20.0 μg L^{-1} range, so the concentration used was 100 μg L^{-1}, as a compromise between the actual concentration in real effluents and the amount required for adequate UPLC analysis sensitivity. Similarly, for sake of simplicity, at least at the beginning, real effluents from MWTP were not used until the photoactivity of the new photocatalyst could be proven adequate.

4.1. Evaluation of the catalyst in a solar simulator

So at the beginning, the spheres were inserted in the reactor and washed several times with distilled water to eliminate non-

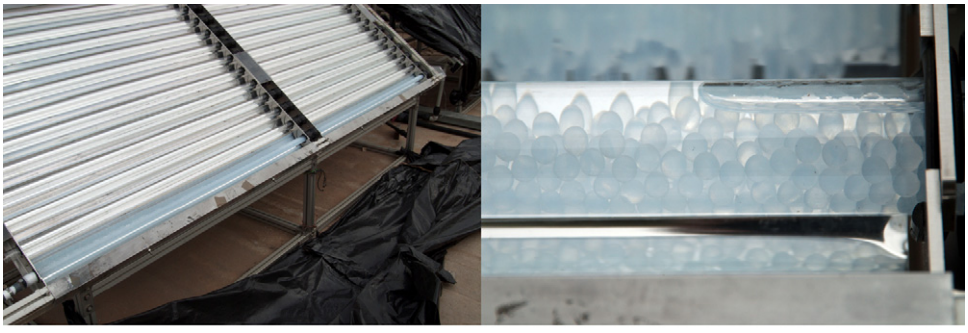

(a) (b)

Fig. 2. CPCs prepared for tests with immobilized TiO_2. (a) General view of the CPCs and (b) detail of one absorber tube filled with the TiO_2 coated spheres shown in Fig. 1.

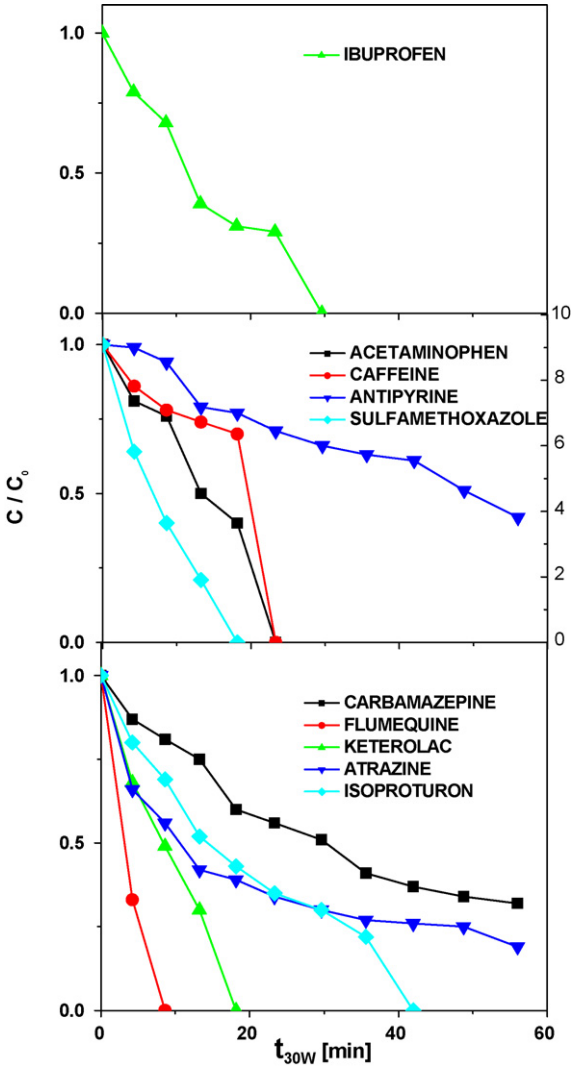

Fig. 3. Degradation of 15 ECs (100 μg L^{-1}) with immobilized TiO_2 in distilled water in the solar simulator. Results are not shown for Hydroxybiphenyl, Dichlofenac, Progesterone, Triclosan and Ofloxacin, as they had already disappeared before the first sample was taken.

bonding or weakly bonded TiO_2 and to avoid any effect produced by TiO_2 particles (released from the immobilized photocatalyst) in suspension. Fig. 3 shows the degradation of the 15 selected ECs (see Fig. 1) at a power of 68.85 W m^{-2} in the UV range (290–400 nm). Before switching on the lamp, the water containing ECs was recirculated 15 min to determine whether there was any adsorption of ECs on photocatalyst. No adsorption was detected. The normalized irradiation time (t_{30W}) necessary to achieve degradation below the LOQ was <5 min for Hydroxybiphenyl, Diclofenac, Progesterone, Triclosan and Ofloxacin, 10 min for Flumequine, around 20 min for Acetaminophen, Caffeine, Sulfamethoxazole and Ketorolac, and 40 min for Ibuprofen and Isoproturon. But after 60 min, Antipyrine, Atrazine and Carbamazepine were still present in significant concentrations (20 μg L^{-1} Atrazine, 30 μg L^{-1} Carbamazepine and 40 μg L^{-1} Antipyrine). The organic content of the water was mainly due to the methanol used in the preparation of the EC mixture, but it should be mentioned that it was also reduced from 13 to 7 mg L^{-1}, demonstrating that the immobilized catalyst was also able to mineralize a significant part of the organic load. This experiment was repeated twice to find out the durability of the immobilized catalyst and the repeatability of the results. All the results were quite similar. The pH varied from 7.06 to 5.14.

In view of these results, and taking into account that in the solar simulator at maximum power (68.85 W m^{-2} in the UV range, about 75–100% more than solar UV radiation on a sunny day) the immobilized photocatalyst was able to substantially degrade the ECs in <1 h of illumination, experimentation was continued in the CPCs solar pilot plant.

4.2. Solar photocatalysis

After the durability and photoactivity of the catalyst had been verified, a second set of the experiments was performed in the CPCs, first with TiO_2 (5 mg L^{-1}) in slurry; followed by a series of five cycles with the same catalyst, but this time immobilized, to compare the efficiency of the immobilized catalyst with a low concentration in suspension. As around 0.5 mg of TiO_2/sphere was immobilized, and 6700 spheres were placed in 2.050 L (1.025 L per photoreactor tube), the comparative quantity of catalyst in suspension would be 3.35 g in 10 L of photoreactor, or 0.335 g L^{-1}). But as the immobilized photocatalyst was only in the illuminated part of the pilot plant (1.92 L) and TiO_2 in slurry was in the complete volume (10 L), the concentration in slurry must be around 5 times higher (1.675 g L^{-1}). This concentration is far from the optimum for this type of photoreactor (0.2 g L^{-1}) and could provoke substantial adsorption of ECs at low concentration, thereby masking the true photocatalytic degradation. Therefore, a comparison of the immobilized and suspended photocatalysts based on the catalyst mass on the spheres would not provide consistent results.

Accordingly, a low TiO_2 concentration (5 mg L^{-1}) was used with the intention of (i) avoiding adsorption of ECs for better comparison of the kinetics; (ii) determining whether results with immobilized photocatalysts were similar to low-concentration slurries; and (iii) determining the stability of the immobilized photocatalyst after several runs.

It should be mentioned that kinetics would be slower with TiO_2 at 5 mg L^{-1} than with the optimized TiO_2 slurry concentration, as only around 10% of the photons could be absorbed in a 30-mm diameter photoreactor [36], but comparison with less efficient TiO_2 slurry at 5 mg L^{-1} was considered more realistic. The suspended TiO_2 experiment showed almost complete degradation of the 15 compounds (Fig. 4) except Atrazine, Antipyrine and Progesterone after 90 min illumination. Degradation followed typical first order kinetics (see Table 2). Organic content was also lowered from 13 to 10 mg L^{-1}.

For the TiO_2 in suspension, the pH varied from 7.06 to 5.13, and in the case of immobilized TiO_2 the initial pH was 5.24 and the final pH was 4.22. In the first run (Fig. 4, right) with immobilized TiO_2, most of the ECs were degraded in $<t_{30W} = 60$ min of irradiation time, except Antipyrine and Sulfamethoxazole. Only Ofloxacin behaves differently, because of adsorption on both slurry and immobilized TiO_2. Flumequine was degraded very quickly in all cases, while Atrazine was the most persistent. It is also important to note that it was not possible to determine any specific tendency common to all ECs during TiO_2 slurry and immobilized TiO_2 experiments. Some ECs are degraded better by the slurry and others by the immobilized catalysts. Some ECs are degraded faster during the first cycle and others during the fifth. This rather inconsistent behavior is related to the low-concentration tested. It could therefore be concluded that the efficiency of the immobilized photocatalyst was quite similar to the slurry and that the immobilized photocatalyst was not deactivated during the any of the cycles.

4.3. Immobilized TiO_2 stability after five cycles

The results of the degradation of the 15 ECs after five cycles under illumination may be observed in Fig. 5.

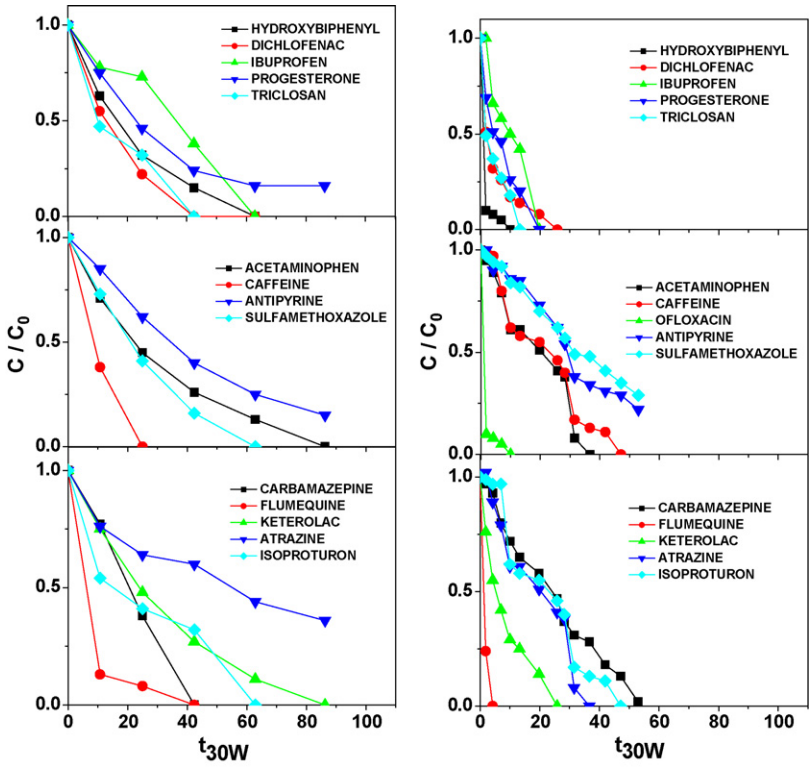

Fig. 4. Degradation of 15 ECs with TiO_2 at 5 mg L^{-1} (left) and with immobilized TiO_2 (right) during the first cycle.

In the last cycle, in which conditions were the same as in the other experiments, degradation of most of the compounds was complete after an illumination time of <60 min, while Acetaminophen was not removed until t_{30W} = 100 min. Atrazine and Antipyrine were more resistant to degradation in all experiments. From the results presented in Table 3, it can be concluded that the continuous use of the immobilized photocatalyst did not reduce its effectiveness. It is interesting to note that after the fifth cycle, Ofloxacin was not as adsorbed on the immobilized photocatalyst, probably due to diminishing active sites on TiO_2 because of adsorption of degradation intermediates. It is therefore important to consider that prolonged use could diminish its effectiveness. One way of avoiding this could be to operate the immobilized photocatalyst with clean water occasionally in order to completely degrade any adsorbed organics.

4.4. TiO_2 coated characterization comparison

Considering that formation of large-sized P25 aggregates can lead to formation of cracks [37] which may have a detrimental effect on the long-term mechanical stability of such films in water treatment applications, particle agglomeration and overall surface morphology of the TiO_2–P25 composite films were examined by SEM. Fig. 6 shows SEM images of the surface of the prepared catalyst, (A) glass sphere surface before use, and (B) after five cycles of heterogeneous photocatalysis. Similar to previously published studies [26,38,39], the TiO_2–P25 composite films showed a rough surface morphology, which included the presence of aggregates composed of P25 nanoparticles. The images show that before and after water treatment, the catalyst surface is rough where broken particles of TiO_2 can been observed, giving the surface a

Table 2
First order and zero order kinetics and illumination time for 90% degradation of the original EC concentration in TiO_2 slurry (5 mg L^{-1} TiO_2) and immobilized TiO_2 (first cycle).

Emerging contaminant	TiO_2, 5 mg L^{-1}			Immobilized TiO_2 (1st cycle)		
	$t_{30W,90\%}$ (min)	k (min^{-1})	R^2 (*order 0)	$t_{30W,90\%}$ (min)	k (min^{-1})	R^2 (*order 0)
Acetaminophen	74.6	0.027	1	31.5	0.080	0.9*
Caffeine	17.9	0.054	-	41.91	0.053	0.9*
Ofloxacin	–	–	0.99	1.9	1.577	0.99
Antipyrine	99.35	0.019	0.99	–	–	–
Sulfamethoxazole	52.62	0.035	0.99	–	–	–
Carbamazepine	33.7	0.029	0.99	47.1	0.083	0.9*
Flumequine	17.9	0.141	0.999	3.1	0.460	0.99*
Keterolac	62.9	0.035	0.9	22.9	0.086	0.9
Atrazine	–	–	0.9	31.5	0.080	0.9*
Isoproturon	78.5	0.015	0.9	41.9	0.053	0.9*
Hydroxybiphenyl	74.6	0.025	0.9	1.9	1.577	0.99
Diclofenac	52.65	0.029	0.99	19.8	0.127	0.9
Ibuprofen	74.6	0.013	0.9*	18.14	0.048	0.9*
Progesterone	–	–	–	22.79	0.071	0.9
Triclosan	52.65	0.022	0.9	16.51	0.104	0.9

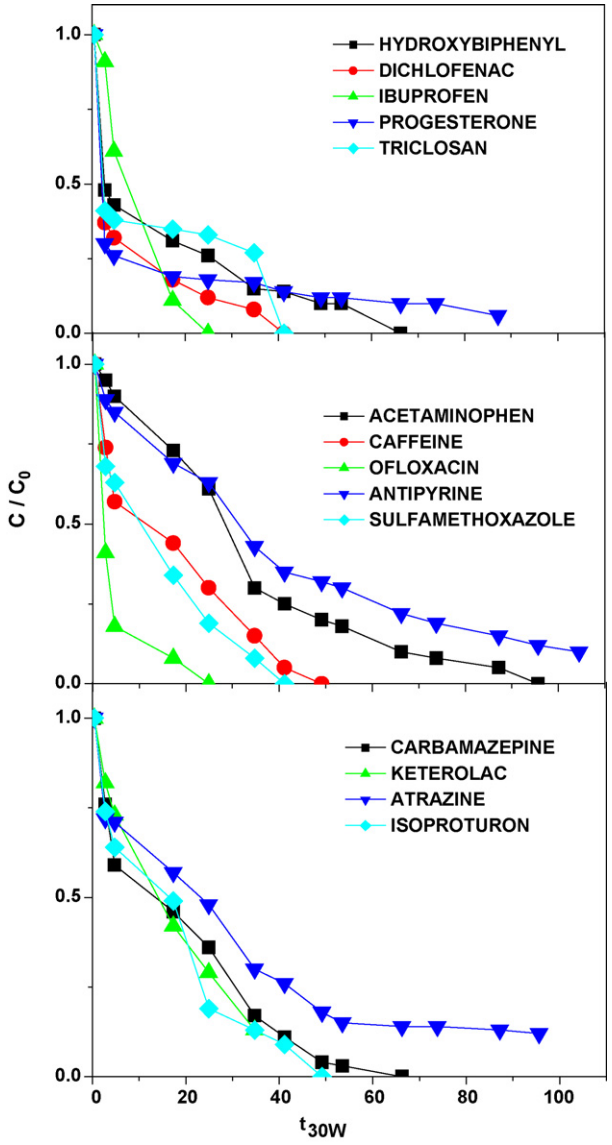

Fig. 5. Degradation of 15 contaminants using the same immobilized TiO_2 (fifth cycle). Results are not shown for Flumequine as it disappeared before the first sample was taken.

granular appearance. As shown, after five treatment cycles, the sphere surface still retains TiO_2 particles, so catalyst preparation by the sol–gel method seems to have provided adequate mechanical resistance.

Table 3
First order kinetics and illumination time for 90% degradation of the original EC concentration with immobilized TiO_2 (fifth cycle).

Emerging contaminant	Immobilized TiO_2 (fifth cycle)		
	$t_{30\,W,90\%}$ (min)	k (min^{-1})	R^2
Acetaminophen	66.24	0.045	0.9
Caffeine	37.95	0.079	0.9
Ofloxacin	11.06	0.228	0.99
Antipyrine	104.41	0.022	0.99
Sulfamethoxazole	29.84	0.085	0.9
Carbamazepine	41.15	0.085	0.9
Flumequine	–	–	–
Keterolac	–	–	–
Atrazine	29.84	0.071	0.9
Isoproturon	41.15	0.059	0.9
Hydroxybiphenyl	49.15	0.047	0.9
Diclofenac	29.84	0.085	0.9
Ibuprofen	17.33	0.127	0.9
Progesterone	–	–	–
Triclosan[a]	66.24	0.019	–

[a]Triclosan kinetic does not correspond at any classical model.

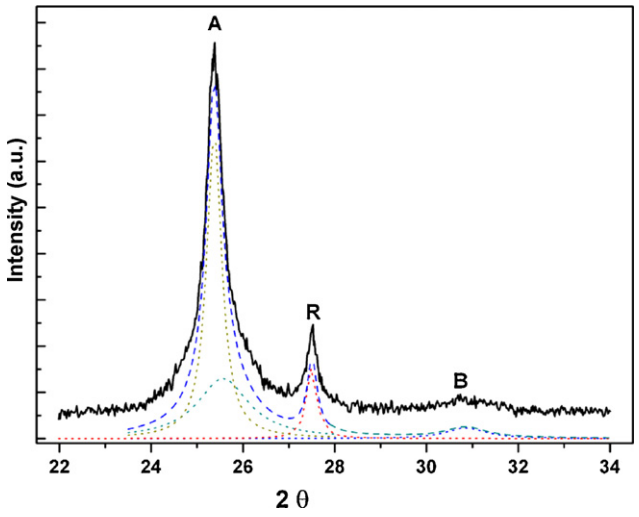

Fig. 7. XRD powder pattern of the photocatalyst calcined at 400 °C (solid) showing the most intense peaks of the TiO_2 anatase (A), rutile (R) and Brookite (B) phases. The dotted curve represents the simulated pattern and the dotted lines show the four lorentzian contributions obtained by deconvolution.

Similar to other immobilized photocatalysts previously used for water treatment [26], the coating developed for this study employed sol–gel TiO_2 as a binder for fixing commercial P25 powders to the glass surface. As revealed by the XRD patterns displayed in Fig. 7, the deposited TiO_2 consists of a mixture of anatase, rutile

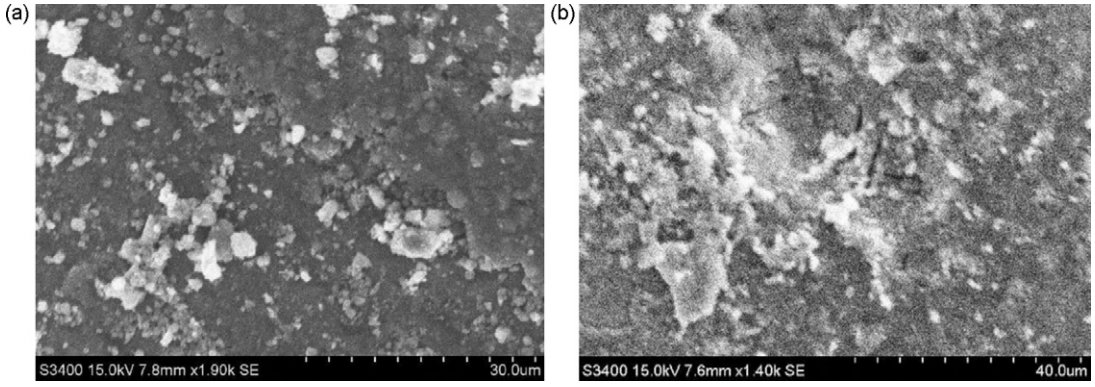

Fig. 6. SEM images of the catalyst surface (a) before use and (b) after five treatment cycles.

and brookite. Using the empirical equations proposed by Zhang and Banfield [40] the proportion between the TiO_2 phases is 78% anatase, 12% rutile and 10% brookite. Close examination of the most intense anatase reflection with (1 0 1) planes, reveals that it consists of two contributions of anatase crystallites of different sizes (see Fig. 7). According to the Scherrer equation, rutile crystallites have an average diameter of 30.3 nm, while anatase bimodal distribution has 20.7 and 5.2 nm crystals, and brookite has 5.3 nm diameter crystals. Considering that the characterization of TiO_2 films prepared under similar conditions is formed by anatase and brookite nanoparticles with an average diameter of <8 nm [32], and in keeping with the preparation route of theses samples, it is suggested that films are formed by relatively large anatase and rutile particles of P25 embedded in a matrix formed by anatase nanoparticles and a minor amount of brookite crystallites. During calcination at 400 °C, the small anatase domains in the sol–gel TiO_2 matrix grow, as reported by Chao et al. [41], providing consistency to the films. On the other hand, it is worth noting that the presence of theses different TiO_2 phases in close contact could favor charge separation, thereby enhancing photoactivity, as frequently suggested [42].

5. Conclusions

The experiments showed that emerging contaminants at low concentrations can be successfully degraded to a few $\mu g\,L^{-1}$, which is negligible, with immobilized TiO_2 under solar irradiation. The removal percentage is between 100% in most of the compounds and 70% of the sulfamethoxazole and atrazine. The degradation rate was similar to TiO_2 slurry at a low concentration, which is an important issue for immobilised photocatalysts as they are usually much less efficient than slurries. Usually, the main limitation of immobilised photocatalysts is not only the low degradation rate but the stability of the film during prolonged use which leads to loss of photoactivity. Impregnation of spheres by the sol–gel method leaves a rough cracked surface, but after five treatment cycles, photoactivity was not significantly decreased.

Acknowledgments

The authors wish to thank the Spanish Ministry of Science and Innovation under the Consolider-Ingenio 2010 Programme (Project CSD 2006-00044 TRAGUA; http://www.consolider-tragua.com), and Noelia Miranda would to thank CIEMAT for her PhD. research grant. The author also wishes to thank Mrs. Deborah Fuldauer for English language correction.

References

[1] R. Hochstrat, T. Witgens, T. Melin, P. Jeffrey, Water Supply 5 (1) (2005) 67.
[2] M.S. Diaz-Cruz, D. Barceló, Chemosphere 72 (3) (2008) 333.
[3] J.B. Rose, Water Sci. Technol. 55 (1–2) (2007) 275.
[4] T. Witgens, F. Salehi, R. Hochstrat, T. Melin, Water Sci. Technol. 57 (1) (2008) 99.
[5] J. Radjenovic, M. Petrovic, D. Barceló, TrAc-Trend Anal. Chem. 26 (11) (2007) 1132.
[6] S.S. Teske, R. Arnold, Rev. Environ. Sci. Biotechnol. 7 (2) (2008) 107.
[7] S.D. Richardson, Anal. Chem. 79 (2007) 4295.
[8] M. Petrovic, S. Gónzalez, D. Barceló, TrAc-Trend Anal. Chem. 22 (2003) 685.
[9] S.D. Richardson, Anal. Chem. 80 (2008) 4373.
[10] M.D. Hernando, M.J. Gómez, A. Agüera, A.R. Fernández-Alba, TrAc-Trend Anal. Chem. 26 (6) (2007) 581.
[11] B. Kasprzyk-Horden, R.M. Dinsdale, A.J. Guwy, Water Res. 42 (13) (2008) 3498.
[12] S.D. Kim, J. Cho, I.S. Kim, B.J. Vanderford, S.A. Snyder, Water Res. 41 (5) (2007) 1013.
[13] M.J. Gómez, M.J. Martínez-Bueno, S. Lacorte, A.R. Fernández-Alba, A. Agüera, Chemosphere 66 (2007) 993.
[14] M.J. Martínez-Bueno, A. Agüera, M.J. Gómez, M.D. Hernando, J.F. García-Reyes, A.R. Fernández-Alba, Anal. Chem. 79 (2007) 9372.
[15] N. Bolong, A.F. Ismail, M.R. Salim, T. Matsura, Desalination 239 (2009) 229.
[16] V. Belgiorno, L. Rizzo, D. Fatta, C.D. Roca, G. Lofrano, A. Nikolaou, V. Naddeo, S. Meric, Desalination 215 (2007) 166.
[17] P.R. Gogate, A.B. Pandit, Adv. Environ. Res. 8 (2004) 501.
[18] K. Ikehata, M.G. El-Din, J. Environ. Eng. Sci. 5 (2006) 81.
[19] I. Gültekin, N.H. Ince, J. Environ. Manage. 86 (2007) 816.
[20] B. Ning, N. Graham, Y. Zhang, M.G. Nakonechny, Ozone-Sci. Eng. 29 (2007) 153.
[21] S. Malato, P. Fernández-Ibáñez, M.I. Maldonado, J. Blanco, W. Gernjak, Catal. Today 147 (2009) 1.
[22] V. Augugliaro, M. Litter, L. Palmisano, J. Soria, J. Photochem. Photobio. C.: Photochem. Rev. 7 (2007) 123.
[23] M. Keshmiri, M. Mohseni, T. Troczynski, Appl. Catal. B: Environ. 53 (2004) 209.
[24] T. Kemmitt, N.I. Al-Salim, M. Waterland, V.J. Kennedy, A. Markwitz, Curr. Appl. Phys. 4 (2004) 189.
[25] I.N. Marttyyanov, K.J. Klabunde, J. Catal. 225 (2004) 408.
[26] G. Balasubramanian, D.D. Dionysiou, M.T. Suidan, I. Baudin, J.M. Laine, Appl. Catal. B: Environ. 47 (2004) 73.
[27] H. Choi, E. Stathatos, D.D. Dionysiou, Appl. Catal. B: Environ. 63 (2006) 60.
[28] J.C. Yu, L. Zhang, J. Yu, Chem. Mater. 14 (2002) 4647.
[29] H. Choi, E. Stathatos, D.D. Dionysiou, Thin Solid Films 510 (2006) 107.
[30] N. Arconada, A. Durán, S. Suárez, R. Portela, J.M. Coronado, B. Sánchez, Y. Castro, Appl. Catal. B: Environ. 86 (2009) 1.
[31] A. Mills, G. Hill, S. Bhopal, I.P. Parkin, S.A. O'Neill, J. Photochem. Photobiol. A: Chem. 160 (2003) 185.
[32] R. Portela, B. Sánchez, J.M. Coronado, R. Caudal, S. Suárez, Catal. Today 129 (2007) 223.
[33] A. Sirisuk, C.G. Hill, M.A. Anderson, Catal. Today 54 (1999) 159.
[34] M. Kositzi, I. Poulios, S. Malato, J. Cáceres, A. Campos, Water Res. 38 (2004) 1147.
[35] N. Klamerth, L. Rizzo, S. Malato, M.I. Maldonado, A. Agüera, A.R. Fernández-Alba, Water Res. 43 (2) (2009) 441.
[36] S. Malato, J. Blanco, M.I. Maldonado, P. Fernández-Ibáñez, D. Alarcón, M. Collares, J. Farinha, J. Correia de Oliviera, Sol. Energy 77 (2004) 513.
[37] Y.J. Chen, D.D. Dionysiou, Appl. Catal. B: Environ. 62 (2006) 255.
[38] Y.J. Chen, D.D. Dionysiou, J. Mol. Catal. A: Chem. 244 (2006) 73.
[39] Y.C. Chen, D.D. Dionysiou, Appl. Catal. A: Gen. 318 (2007) 129.
[40] H. Zhang, J.F. Banfield, J. Phys. Chem. B 104 (2000) 3481.
[41] H.E. Chao, Y.U. Yun, H.U. Xingfang, A. Larbot, J. Eur. Ceram. Soc. 23 (2003) 1457.
[42] R.I. Bickely, T. González-Carreño, J.S. Lees, L. Palmisano, R.I. Tilley, J. Solid-State Chem. 92 (1991) 178.